

Alicyclic Polyimides with Large Bandgap Exhibiting Superior High-Temperature Capacitive Energy Storage

Jinhui Song,^a Hongmei Qin,^a Shiyu Qin,^a Man Liu,^a Shixian Zhang,^a Junyu Chen,^a
Yang Zhang,^a Shan Wang,^{*a} Qi Li,^{*b} Lijie Dong^{*a} and Chuanxi Xiong^a

^a School of Materials Science and Engineering, Wuhan University of Technology,
Wuhan, 430070, China

^b State Key Laboratory of Power System, Department of Electrical Engineering,
Tsinghua University, Beijing 100084, China

* Corresponding authors

Email: shanwang@whut.edu.cn; qili1020@tsinghua.edu.cn; dong@whut.edu.cn

1. DFT calculation

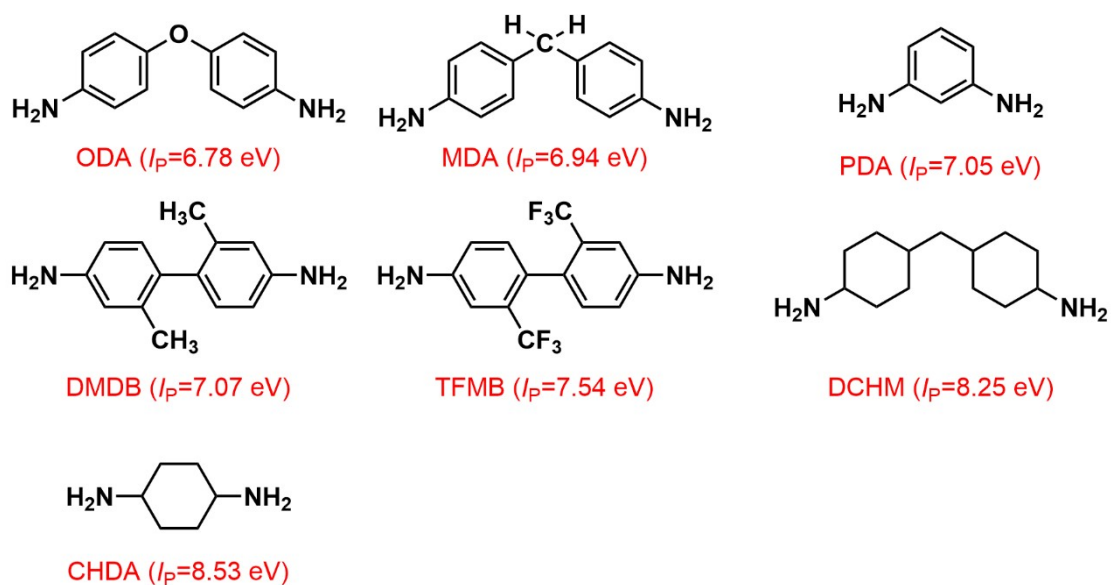


Figure S1. Structures of diamines and their ionization potentials (I_p) calculated by the density functional theory at the B3LYP/6-311G(d,p) level.

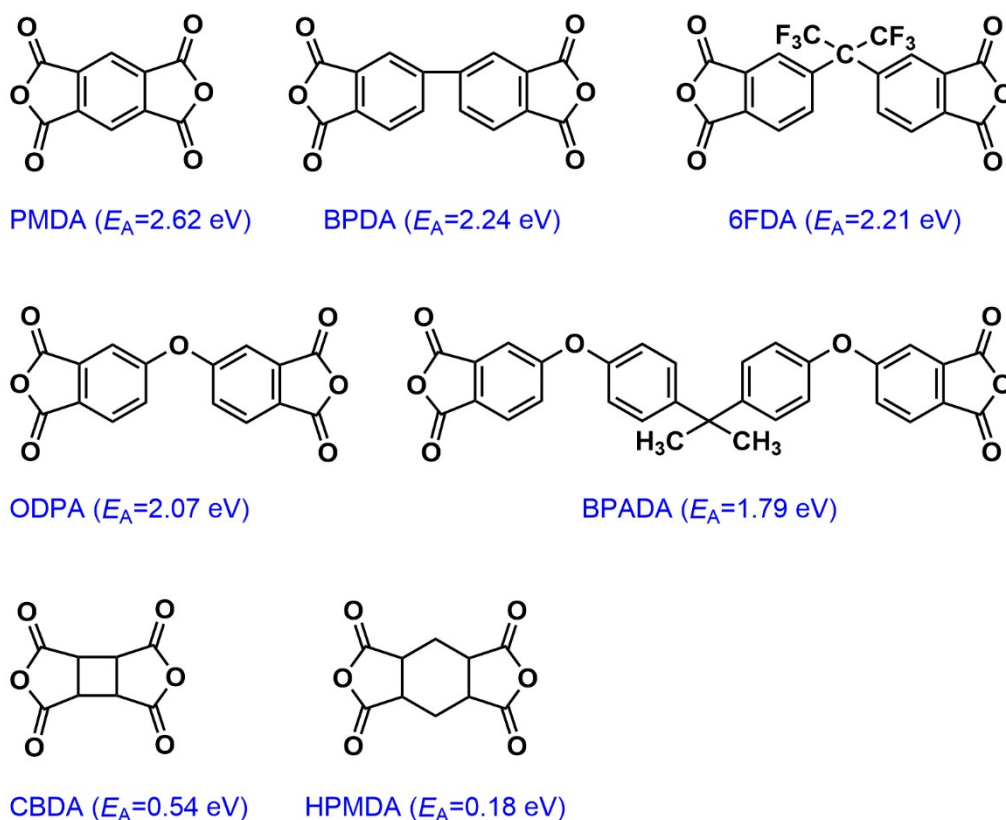
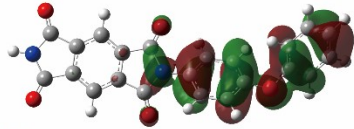
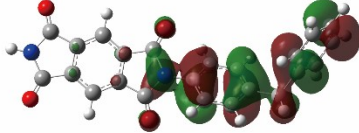


Figure S2. Structures of dianhydrides and their electron affinities (E_A) calculated by the density functional theory at the B3LYP/6-311G(d,p) level.

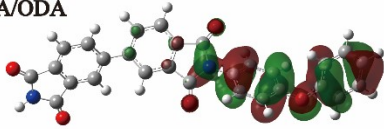
PMDA/ODA **HOMO**



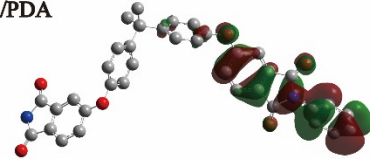
PMDA/MDA



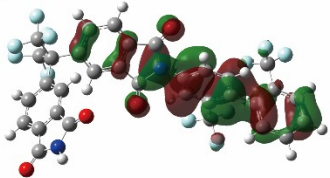
BPDA/ODA



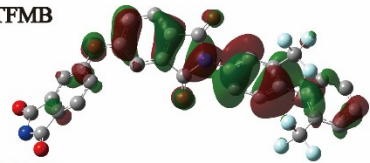
BPADA/PDA



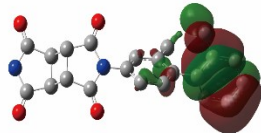
6FDA/TFMB



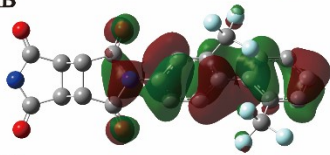
ODPA/TFMB



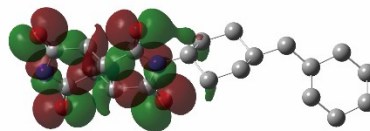
CBDA/DMDB



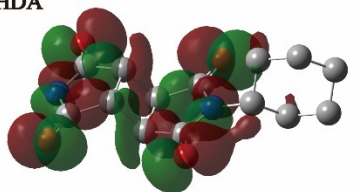
CBDA/TFMB



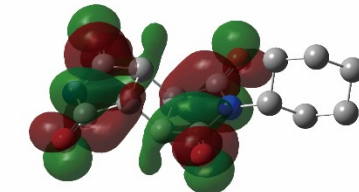
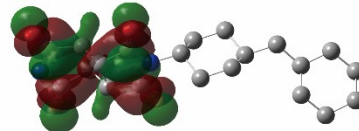
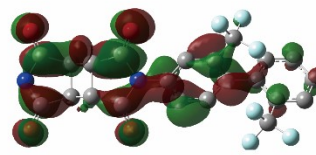
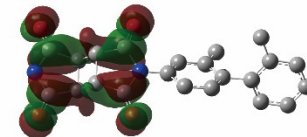
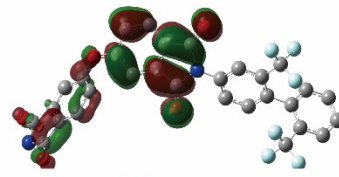
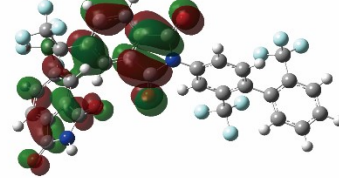
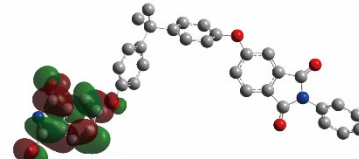
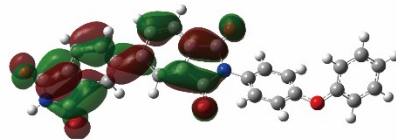
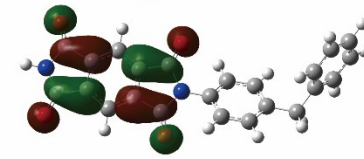
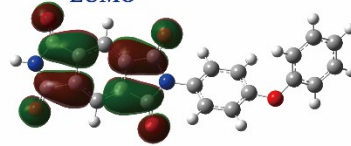
CBDA/DCHM



CBDA/CHDA



LUMO



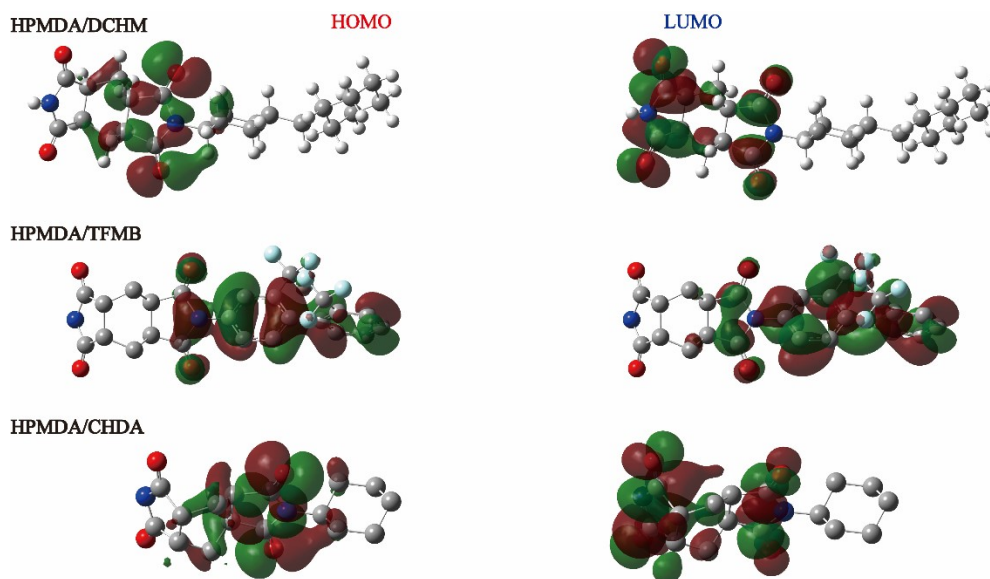


Figure S3. Spatial distributions of the HOMO (left-hand side) and LUMO (right-hand side) of PI model compounds.

Table S1. Summarization of the HOMO (E_{HOMO}) and LUMO (E_{LUMO}) energy levels of PI model compounds, and the ionization potential (I_{p}) and electron affinity (E_{A}) of the diamine and dianhydride monomers, respectively.

PI model	$E_{\text{HOMO}}/\text{eV}$	$E_{\text{LUMO}}/\text{eV}$	I_{p}/eV	E_{A}/eV
PMDA/ODA	-6.29	-3.48	6.78	2.62
PMDA/MDA	-6.64	-3.42	6.94	2.62
BPDA/ODA	-6.16	-2.95	6.78	2.24
ODPA/TFMB	-6.96	-2.83	7.54	2.07
BPADA/PDA	-6.52	-2.44	7.05	1.79
6FDA/TFMB	-7.08	-3.08	7.54	2.21
CBDA/DMDB	-6.79	-1.45	7.07	0.54
CBDA/TFMB	-7.29	-1.76	7.54	0.54
CBDA/DCHM	-7.46	-1.46	8.25	0.54
CBDA/CHDA	-7.48	-1.47	8.53	0.54
HPMDA/DCHM	-7.33	-1.16	8.25	0.18
HPMDA/TFMB	-7.17	-1.60	7.54	0.18
HPMDA/CHDA	-7.34	-1.16	8.53	0.18

2. Inherent viscosity

The molecular weights of the CBDA/TFMB and CBDA/DCHM were indirectly characterized by measuring the inherent viscosity of their corresponding PAA solution, since they are insoluble in common solvents. The inherent viscosity of the as-prepared PAA solutions (0.5 g/dL) was measured by using a Ubbelohde viscometer at 30 °C and calculated as:

$$\eta_{\text{inh}} = \ln(t/t_0)/C$$

where t_0 and t are the outflow time of the pure solvent and PAA solution with a concentration of 0.5 g/dL, respectively.¹

Table S2. Inherent viscosity of various PAA solutions

PAA type	η_{inh}	Film-forming properties
CBDA/TFMB	2.02 dL g ⁻¹	Good
CBDA/DCHM	1.54 dL g ⁻¹	Good
CBDA/CHDA	0.36 dL g ⁻¹	Brittle
HPMDA/DCHM	0.40 dL g ⁻¹	Brittle
HPMDA/TFMB	0.40 dL g ⁻¹	Brittle
HPMDA/CHDA	0.39 dL g ⁻¹	Brittle

The inherent viscosities of the prepared CBDA/TFMB and CBDA/DCHM are larger than 1 dL g⁻¹, indicating that flexible PI films can be successfully obtained according to previous literature.²

3. Mechanical properties

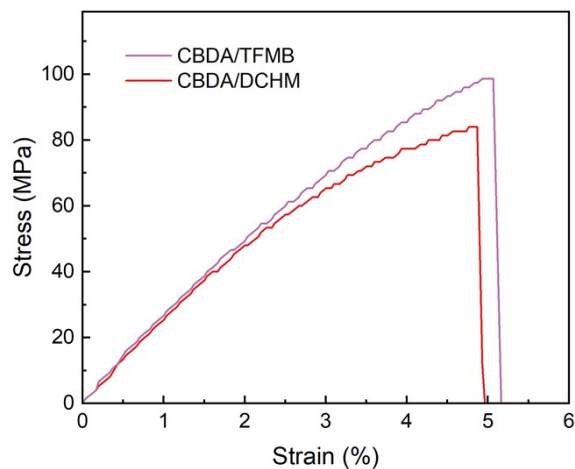


Figure S4. Stress-strain curves of CBDA/TFMB and CBDA/DCHM films.

4. FT-IR and UV-Vis spectroscopy

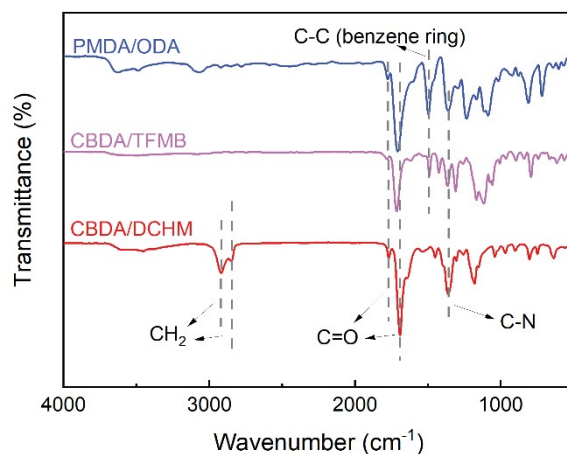


Figure S5. FT-IR spectra of PMDA/ODA, CBDA/TFMB, and CBDA/DCHM films.

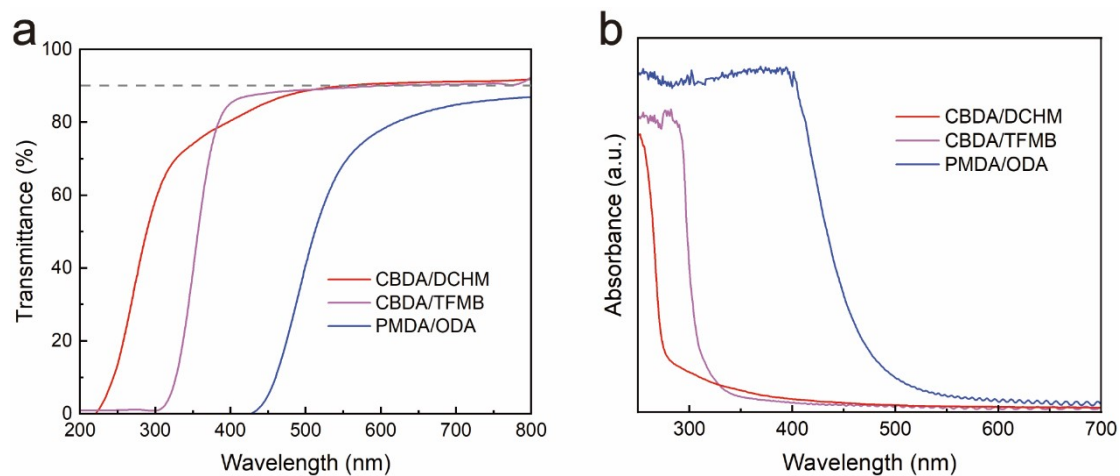


Figure S6. (a) UV-Vis transmission and (b) absorption spectra of PMDA/ODA,

CBDA/TFMB, and CBDA/DCHM films.

5. Thermal properties

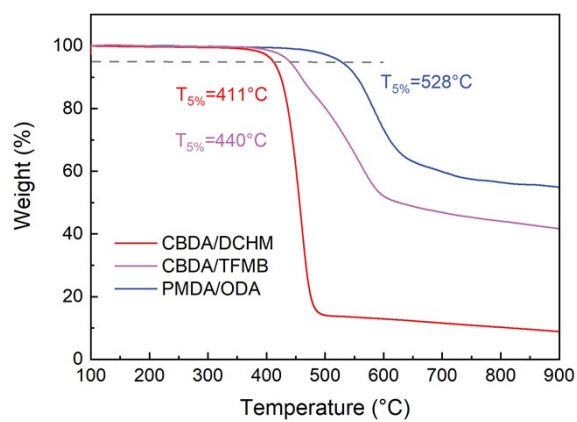


Figure S7. TGA curves of PMDA/ODA, CBDA/TFMB and CBDA/DCHM measured in a nitrogen atmosphere at a heating rate of 10 °C/min.

6. Electrical properties

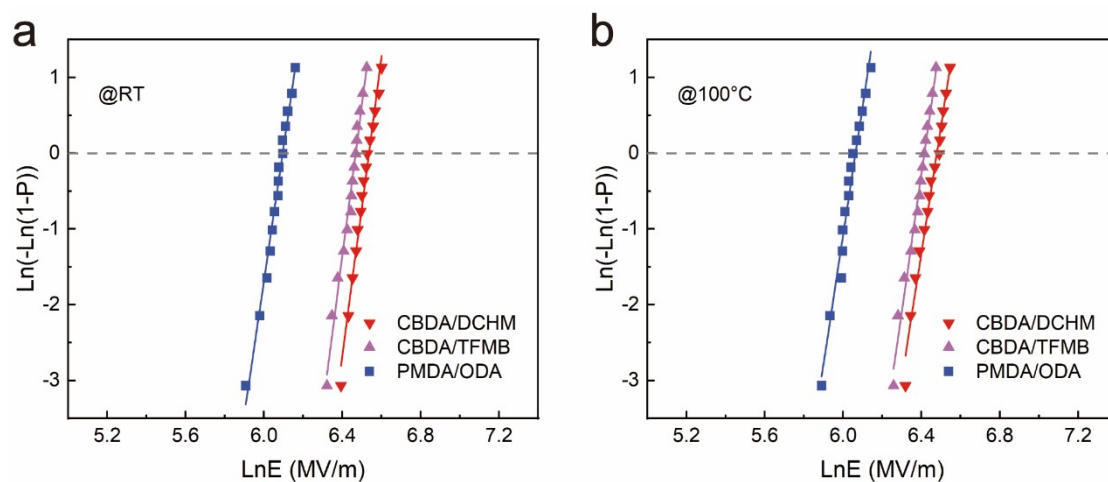


Figure S8. Weibull statistic of dielectric breakdown strength of CBDA/DCHM, CBDA/TFMB, and PMDA/ODA at (a) room temperature and (b) 100 °C.

Table S3. Weibull statistic parameters of CBDA/DCHM, CBDA/TFMB, and PMDA/ODA

Temperature (°C)	Polyimide film	E_b (MV/m)	β
RT	PMDA/ODA	446	18
	CBDA/TFMB	645	20
	CBDA/DCHM	692	20
100 °C	PMDA/ODA	428	17
	CBDA/TFMB	608	18
	CBDA/DCHM	652	17
150 °C	PMDA/ODA	307	9
	CBDA/TFMB	556	13
	CBDA/DCHM	620	12
200 °C	PMDA/ODA	270	6
	CBDA/TFMB	497	9
	CBDA/DCHM	605	10

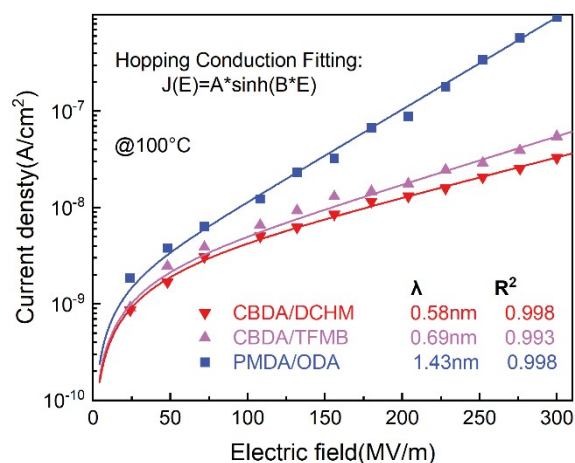


Figure S9. Leakage current density of CBDA/DCHM, CBDA/TFMB, and PMDA/ODA as a function of electric field at 100 °C. Solid lines are the fitting of the hopping conduction model.

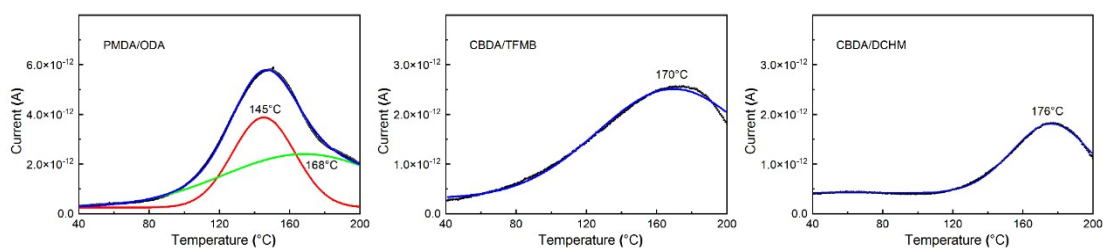


Figure S10. Gaussian fitting of the TSDC spectra of PMDA/ODA, CBDA/TFMB, and CBDA/DCHM.

Table S4. Charge trap parameters of PMDA/ODA, CBDA/TFMB, and CBDA/DCHM derived from the TSDC spectra

Sample	Temperature of Peak (°C)	Activation energy (eV)
PMDA/ODA	145	1.30
	168	1.36
CBDA/TFMB	170	1.37
CBDA/DCHM	176	1.39

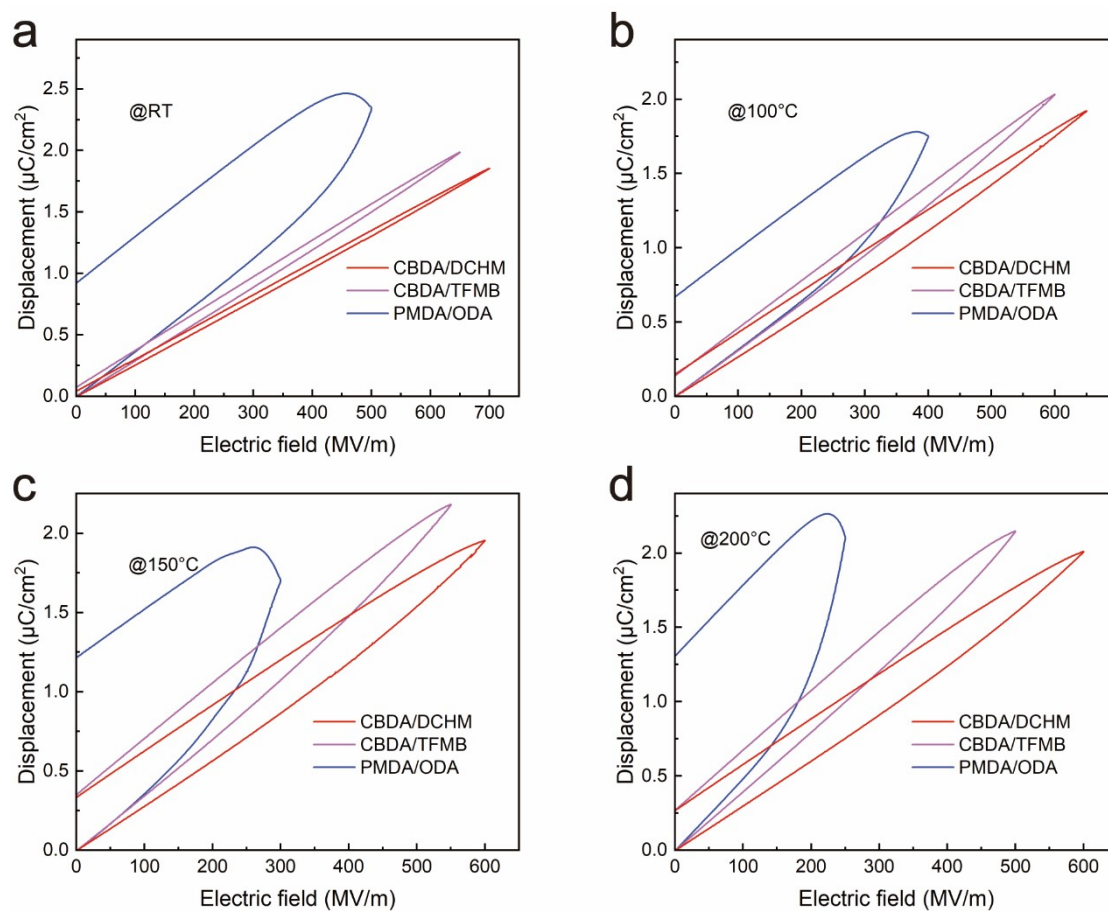


Figure S11. Electric displacement-electric field (D - E) loops of CBDA/DCHM, CBDA/TFMB, and PMDA/ODA measured at (a) room temperature, (b) 100 °C, (c) 150 °C, and (d) 200 °C, at their respective maximum field strength.

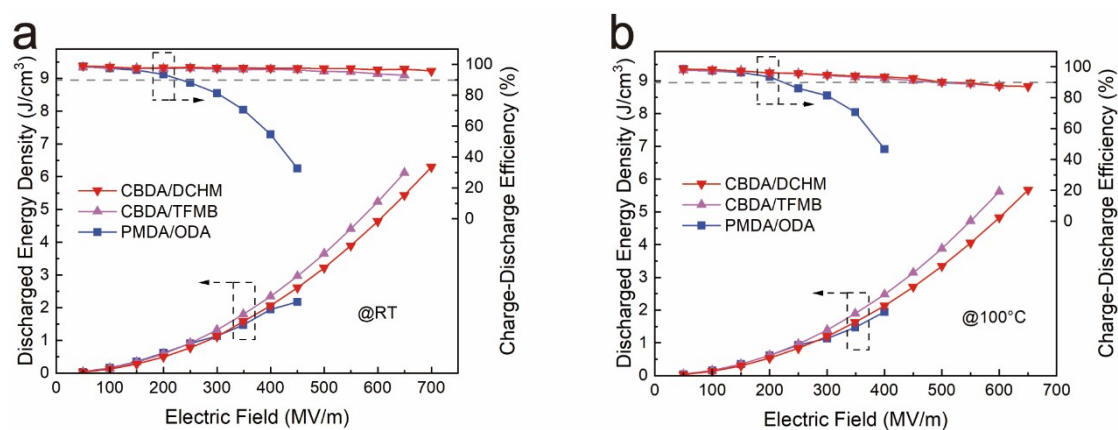


Figure S12. Discharged energy density and charge-discharge efficiency of CBDA/DCHM, CBDA/TFMB, and PMDA/ODA at (a) room temperature and (b) 100 °C.

Reference

- 1 J. Yi, C. Liu, Y. Tian, K. Wang, X. Liu and L. Luo, *Polymer*, 2021, 218, 123488.
- 2 M. Hasegawa, M. Horiuchi, K. Kumakura and J. Koyama, *Polymer international*, 2014, 63, 486-500.